

**Electronic Supplementary Information for:
Singlet and Triplet Energy Transfer Dynamics in
Self-Assembled Axial Porphyrin-Anthracene
Complexes: Towards Supra-molecular Structures
for Photon Upconversion**

Victor Gray, Betül Küçüköz, Fredrik Edhborg, Maria Abrahamsson, Kasper
Moth-Poulsen, and Bo Albinsson*

*Department of Chemistry and Chemical Engineering, Chalmers University of Technology,
Gothenburg, Sweden*

E-mail: balb@chalmers.se

*To whom correspondence should be addressed

Contents

1	Synthesis	S2
1.1	NMR spectra	S7
2	Binding dynamics and SVD analysis	S10
3	Triplet Energy Transfer Dynamics	S12
3.1	Transient Absorption Spectra	S14
3.2	Time resolved Phosphorescence	S15
4	Singlet Energy Transfer	S16
4.1	Förster Resonance Energy Transfer	S16
4.2	Charge Transfer	S18
5	Upconversion Measurements	S18
5.1	Effect of Extending the Triplet Lifetime of the Sensitizer	S19

1 Synthesis

Starting materials were purchased from Sigma-Aldrich or Fisher Scientific and used as received if not stated otherwise. Free-base porphyrin was purchased from PorphyChem. Dry and degassed solvents were obtained using a M-Braun solvent drying system. NMR was run on a 400 MHz Varian NMR. IR was run on a Perkin Elmer ATR-FTIR. Matrix-assisted laser desorption ionization-time of flight mass spectrometry (MALDI-TOF MS) was performed on a Bruker Autoflex. Column chromatography was carried out using a Biotage Flash Column Chromatography system with Biotage prepacked SNAP columns. Melting points were determined using an automatic Mettler Toledo MP70 melting point apparatus.

The preparation of pyridine terminated ligands **2-5** has been reported by us previously.^{S1} Figure S1 shows the synthetic route to the new compounds **1**, **6** and **7**. The two dendrimeric

arms **6** and **7** are similar to the dendrimers studied in our previous work,^{S2,S3} the synthesis of compounds **8** and **9** has been reported previously.^{S2}

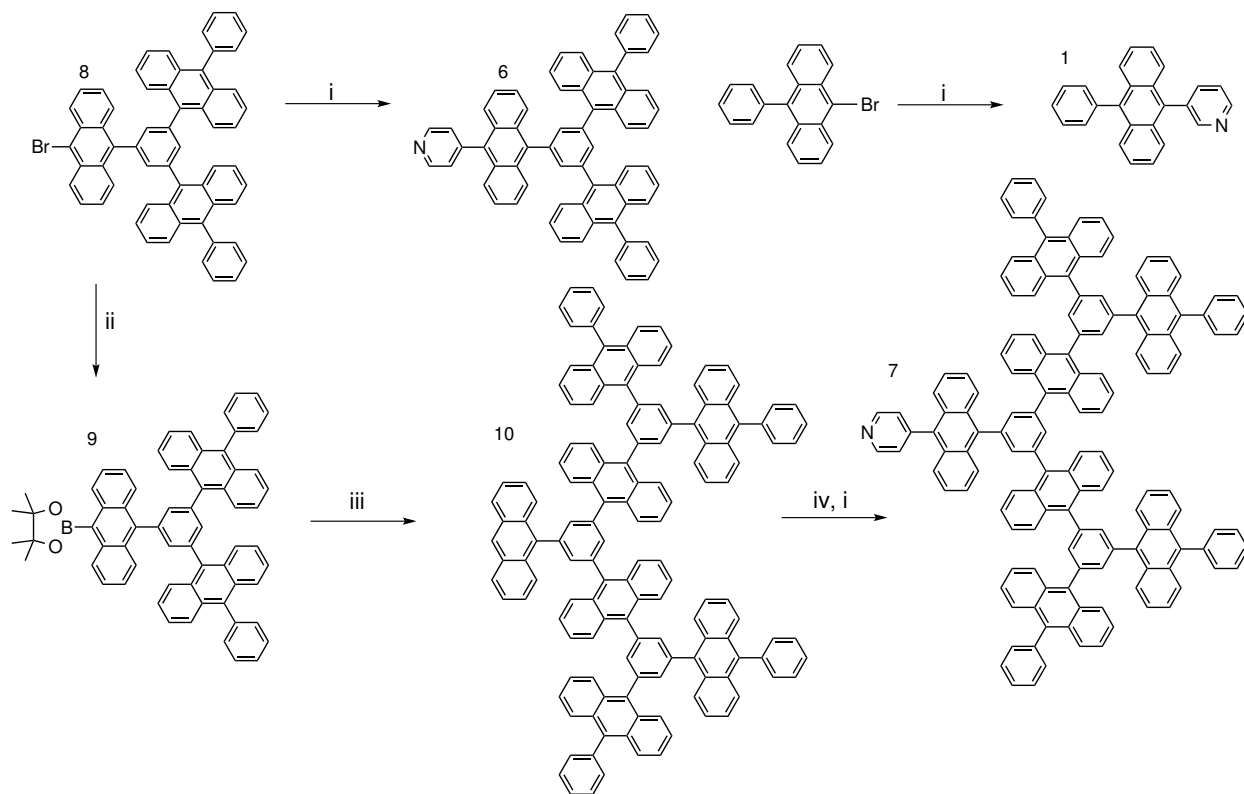


Figure S1: Synthetic route of ligands **2**, **6** and **7**. i) Pyridineboronic acid, Pd(PPh₃)₄, THF, K₂CO₃ (aq. 2M), Aliquat 336. ii) t-BuLi, -78°C 1 h, then 2-isopropoxy-4,4,5,5-tetramethyl-1,3,2-dioxaborolane, -78°C → RT, 16 h. iii) Pd₂(dba)₃, tri-*o*-tolylphosphine, toluene, tetraethylammonium hydroxide (aq, 20%), reflux 72 h. iv) Br₂, CCl₄, 0°C, 1 h.

3-(10-phenylanthracen-9-yl)pyridine, 1 Degassed THF (5.9 ml), toluene (3 ml), a drop of Aliquat 366 and K₂CO₃ (2 M, aq, 6 ml) was added to a reaction vessel containing 9-bromo-10-phenylanthracene (1.20 mmol, 400 mg), 3-pyridineboronic acid (1.32 mmol, 253 mg), Pd(PPh₃)₄ (0.02 mmol, 20 mg). The reaction mixture was refluxed and vigorously stirred for 72 h under nitrogen. The crude product was extracted with DCM. The organic phase was washed twice with water, then with brine and evaporated to dryness. The crude reaction mixture was washed over a plug of silica with DCM and then flushed through with 10% MeOH in DCM, to give **6** in 86% yield. Mp = 235.3°C. ¹H NMR (400 MHz, CDCl₃) δ

= 8.83 (dd, $J_1 = 1.7$ Hz, $J_2 = 4.9$ Hz, 1H), 8.75 (dd, $J_1 = 0.8$ Hz, $J_2 = 2.1$ Hz, 1H), 7.84 (dt, $J_1 = 2.1$ Hz, $J_2 = 7.7$ Hz, 1H), 7.73-7.69 (m, 2H), 7.64-7.54 (m, 6H), 7.50-7.45 (m, 2H), 7.39-7.33 (m, 4H). ^{13}C NMR (100 MHz, CDCl_3) $\delta = 151.85, 148.91, 138.86, 138.74, 138.14, 132.62, 131.21, 131.14, 130.12, 129.82, 128.46, 128.41, 127.60, 127.19, 126.16, 125.59, 125.13, 123.38, 110.34$.

FT-IR (ATR) $\nu(\text{cm}^{-1})$ 3064 (w), 3028 (w), 2925 (w), 1442 (m), 1390 (m), 1026 (m), 942 (m), 814 (w), 766 (s), 730 (m), 716 (w), 703 (s), 663 (m), 610 (w).

MALDI-TOF (m/z): Calculated for $\text{C}_{25}\text{H}_{17}\text{N} = 331.14$, found 331.04

4-(10-(3,5-bis(10-phenylanthracen-9-yl)phenyl)anthracen-9-yl)pyridine, 6 Degassed

THF (1.8 ml), a drop of Aliquat 366 and K_2CO_3 (2 M, aq, 1.8 ml) was added to a reaction vessel containing **8** (0.36 mmol, 300 mg), 4-pyridineboronic acid (0.72 mmol, 88 mg), $\text{Pd}(\text{PPh}_3)_4$ (0.02 mmol, 20 mg). The reaction mixture was refluxed and vigorously stirred for 72 h under nitrogen. The crude product was extracted with DCM. The organic phase was washed twice with water, then with brine and evaporated to dryness. The crude reaction mixture was purified by column chromatography (0-100% DCM in Hexane, $R_f=0.18$ in DCM) and then recrystallized from toluene to give **6** in 78% yield. Mp = 254.8°C. ^1H NMR (400 MHz, CDCl_3) $\delta = 8.87$ (d, $J = 4.4$ Hz, 2H), 8.28 (m, 6H), 7.91 (t, $J = 1.6$ Hz) 7.88 (t, $J = 1.6$ Hz, 2H), 7.71 (dt, $J_1 = 8.5$ Hz $J_2 = 0.7$ Hz, 4H), 7.61-7.52 (m, 14H), 7.49-7.36 (m, 12H). ^{13}C NMR (100 MHz, CDCl_3) $\delta = 150.07, 147.65, 139.37, 138.92, 137.85, 137.60, 137.40, 136.14, 134.19, 134.03, 133.86, 131.26, 130.00, 129.94, 129.87, 129.20, 129.02, 128.40, 128.21, 127.51, 127.25, 126.99, 126.66, 126.55, 126.27, 125.75, 125.68, 125.50, 125.05$.

FT-IR (ATR) $\nu(\text{cm}^{-1})$ 3086 (w), 3061 (m), 3026 (w), 1593 (m), 1520 (w), 1499 (w), 1441 (m), 1403 (w), 1373 (m), 1219 (w), 1176 (w), 1029 (m) 926 (m), 814 (w), 771 (s), 760 (m), 727 (m), 702 (m), 638 (w), 618 (w).

MALDI-TOF (m/z): Calculated for $\text{C}_{65}\text{H}_{41}\text{N} = 835.32$, found 835.25

10,10',10'',10'''-(((5-(anthracen-9-yl)-1,3-phenylene)bis(anthracene-10,9-diyl))bis(benzene-5,1,3-triyl))tetrakis(9-phenylanthracene), 10 Degassed toluene (15 ml) and tetraethylammonium hydroxide (20% aq, 8 ml, 11.6 mmol) was added to a reaction vessel containing 1-anthracene-3,5-bromobenzene (0.29 mmol, 150 mg), **9** (1 mmol, 930 mg), Pd₂(dba)₃ (0.10 mmol, 100 mg) and tri(o-tolyl)phosphine (0.41 mmol, 120 mg). The reaction mixture was refluxed and vigorously stirred for 72 h under nitrogen. The crude product was extracted with toluene. The organic phase was washed twice with water, then with brine and evaporated to dryness. The crude reaction mixture was purified by column chromatography (5-35% DCM in Hexane, *R_f*=0.22 for DCM/Hexane 4:7) to give **10** in 75% yield. ¹H NMR (400 MHz, CDCl₃) δ = 8.47 (s, 1 H), 8.26 (m, 18 H), 8.02 (d, *J* = 8.4 Hz, 2 H), 7.85 (m, 9 H), 7.68 (dd, *J* = 8.8 Hz, *J* = 3.2 Hz, 8 H), 7.62-7.30 (m, 48 H) ¹³C NMR (100 MHz, CDCl₃) δ = 139.26, 139.17, 139.16, 139.00, 138.97, 137.50, 137.49, 136.70, 136.67, 136.26, 136.25, 136.11, 134.07, 133.98, 133.94, 133.88, 131.42, 131.28, 130.26, 130.10, 130.08, 129.98, 129.94, 128.55, 128.39, 127.47, 127.01, 126.73, 126.59, 125.80, 125.47, 125.12, 125.03
MALDI-TOF (*m/z*): Calculated for C₁₄₀H₈₆ = 1766.67, found 1766.15

10,10',10'',10'''-(((5-(10-bromoanthracen-9-yl)-1,3-phenylene)bis(anthracene-10,9-diyl))bis(benzene-5,1,3-triyl))tetrakis(9-phenylanthracene), 11 0.2 ml Br₂ in CCl₄ (0.8 mM, 0.16 mmol) is added to **10** (0.16 mmol, 290 mg) in 35 ml CCl₄ at 0°C. After stirring for 1 h the reaction is extracted with NaHCO₃ and DCM and washed with water. The crude reaction mixture was purified by recrystallization from DCM slowly mixing with MeOH, giving **11** in 98% yield. ¹H NMR (400 MHz, CDCl₃) δ = 8.61 (m, 2 H), 8.26 (m, 18 H), 7.86 (m, 7 H), 7.79 (d, *J* = 1.5 Hz, 2 H), 7.69 (dd, *J* = 8.8 Hz, *J* = 3.2 Hz, 8 H), 7.62-7.30 (m, 48 H) ¹³C NMR (100 MHz, CDCl₃) δ = 139.28, 139.24, 139.07, 138.93, 138.63, 137.48, 137.47, 136.80, 136.35, 136.19, 134.18, 134.06, 133.92, 133.79, 131.25, 131.03, 130.29, 130.05, 130.03, 129.95, 129.94, 129.90, 128.36, 128.08, 127.46, 127.18, 127.09, 127.03, 126.94, 126.83, 126.68, 126.01, 125.58, 125.51, 125.44, 125.00.

MALDI-TOF (m/z): Calculated for C₁₄₀H₈₅Br = 1844.58, found 1845.05

4-(10-(3,5-bis(10-(3,5-bis(10-phenylanthracen-9-yl)phenyl)anthracen-9-yl)phenyl)-anthracen-9-yl)pyridine, 7 Degassed THF (0.8 ml), toluene (0.8 ml) a drop of Aliquat 366 and K₂CO₃ (2 M, aq, 0.4 ml) was added to a reaction vessel containing **11** (0.16 mmol, 300 mg), 4-pyridineboronic acid (0.33 mmol, 40 mg), Pd(PPh₃)₄ (0.005 mmol, 6 mg). The reaction mixture was refluxed and vigorously stirred for 72 h under nitrogen. The crude product was extracted with DCM. The organic phase was washed twice with water, then with brine and evaporated to dryness. The crude reaction mixture was loaded on a silica packed column, eluted with DCM/Hexane (7:3) until the first fraction was obtained, then the product was eluted with pure DCM. The obtained product was then recrystallized from toluene/heptane (1:1) to give **7** in 37% yield. Degrades over 329°C. ¹H NMR (400 MHz, CDCl₃) δ = 8.77, 8.77, 8.76, 8.76, 8.24, 8.17, 7.81, 7.78, 7.63, 7.62, 7.61, 7.60, 7.53, 7.42, 7.39, 7.26. ¹³C NMR (100 MHz, CDCl₃) δ = 150.00, 139.25, 139.08, 138.93, 137.48, 136.77, 136.46, 136.18, 134.06, 133.93, 131.24, 130.06, 129.95, 129.91, 129.83, 129.15, 128.35, 127.48, 127.45, 127.17, 127.02, 126.88, 126.67, 126.50, 126.22, 125.70, 125.66, 125.55, 125.51, 125.42, 124.99, 109.99.

FT-IR (ATR) ν (cm⁻¹) 3080 (m), 3052 (m), 3036 (m), 2922 (w), 2857 (w), 1941 (w), 1815 (w), 1707 (w), 1592 (m), 1520 (m) 1495 (m), 1441 (m), 1406 (w), 1371 (s), 1212 (w), 1177 (w), 1070 (w), 1029 (m), 923 (w), 859 (w), 816 (w), 778 (m), 765 (s), 729 (s), 703 (s), 695 (w), 673 (w), 654 (w), 639 (w), 612 (w), 465 (w), 420 (w).

MALDI-TOF (m/z): Calculated for C₁₄₅H₈₉N = 1844.70, found 1844.93

1.1 NMR spectra

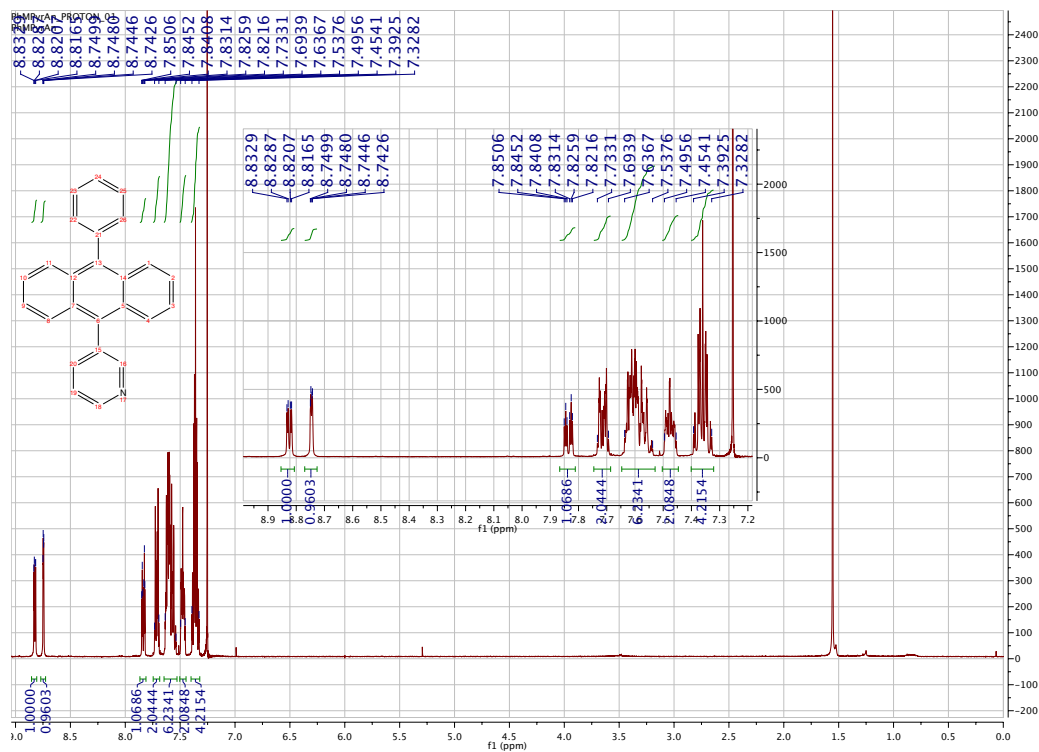


Figure S2: ¹H NMR of **1**

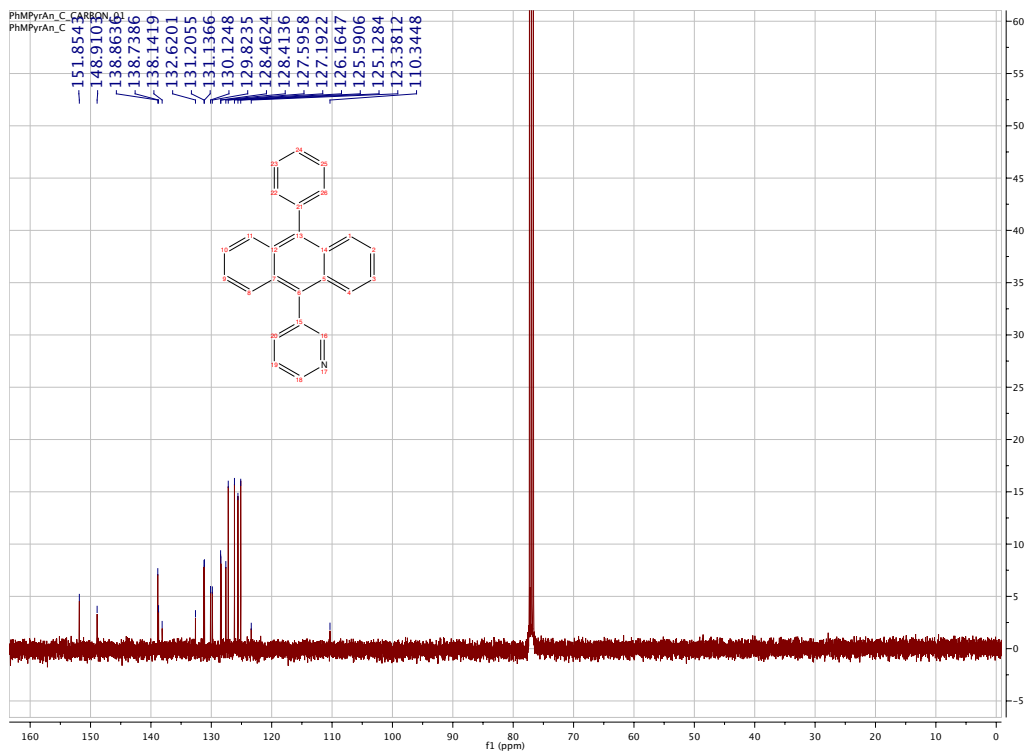


Figure S3: ¹³C NMR of **1**

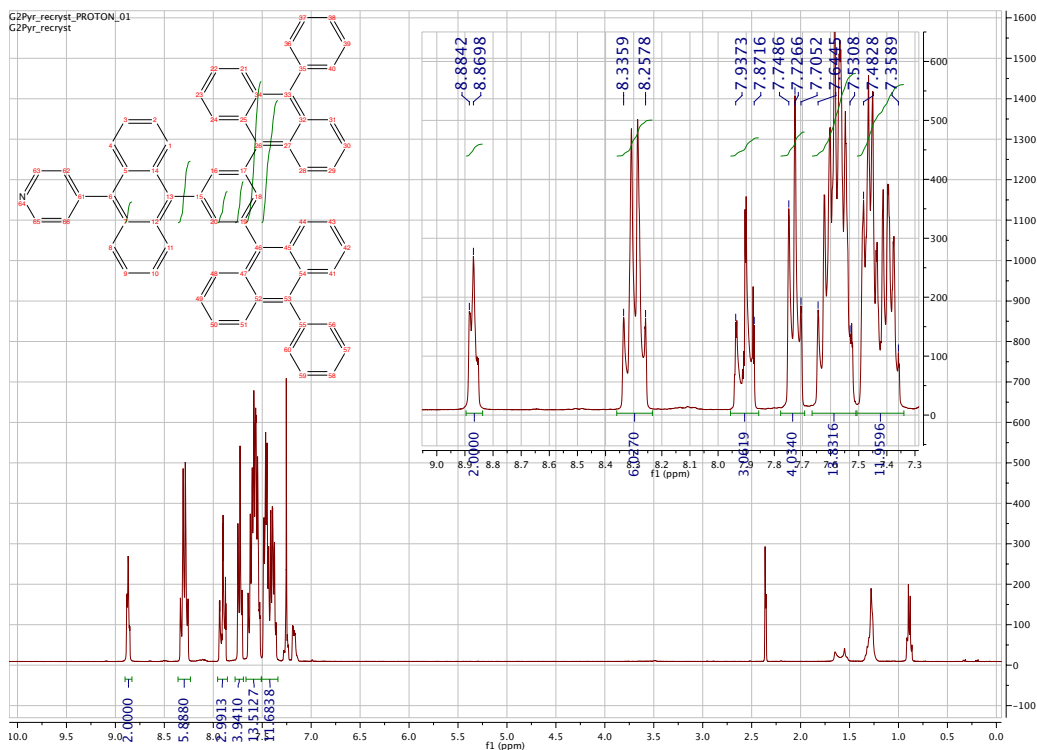


Figure S4: ¹H NMR of **6**

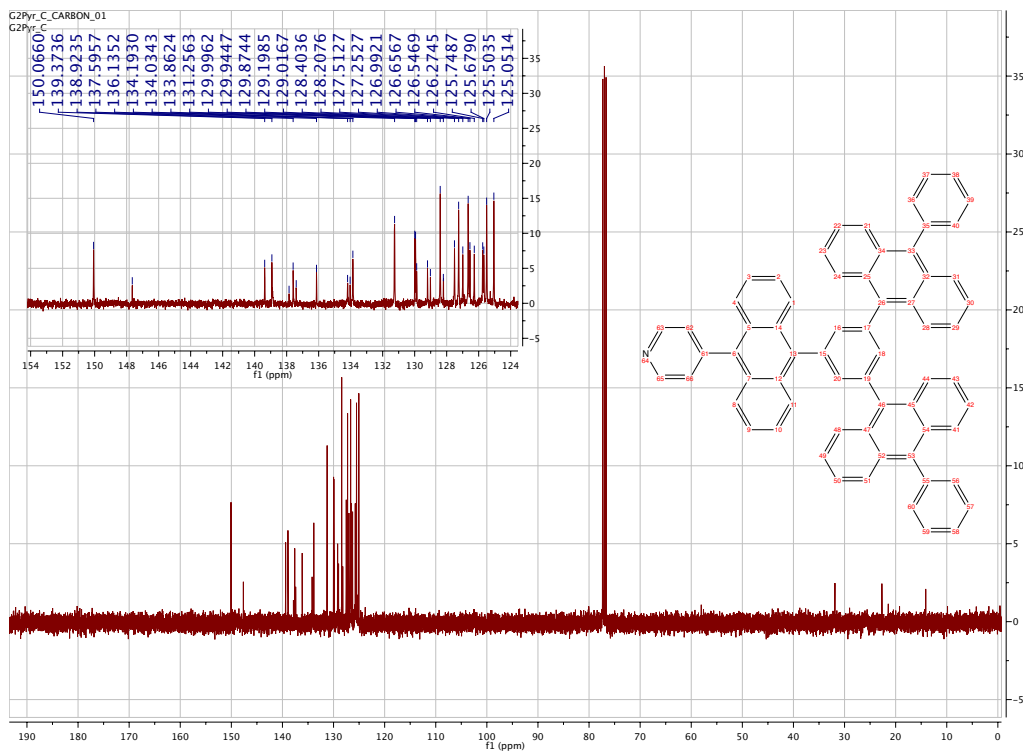


Figure S5: ^{13}C NMR of 6

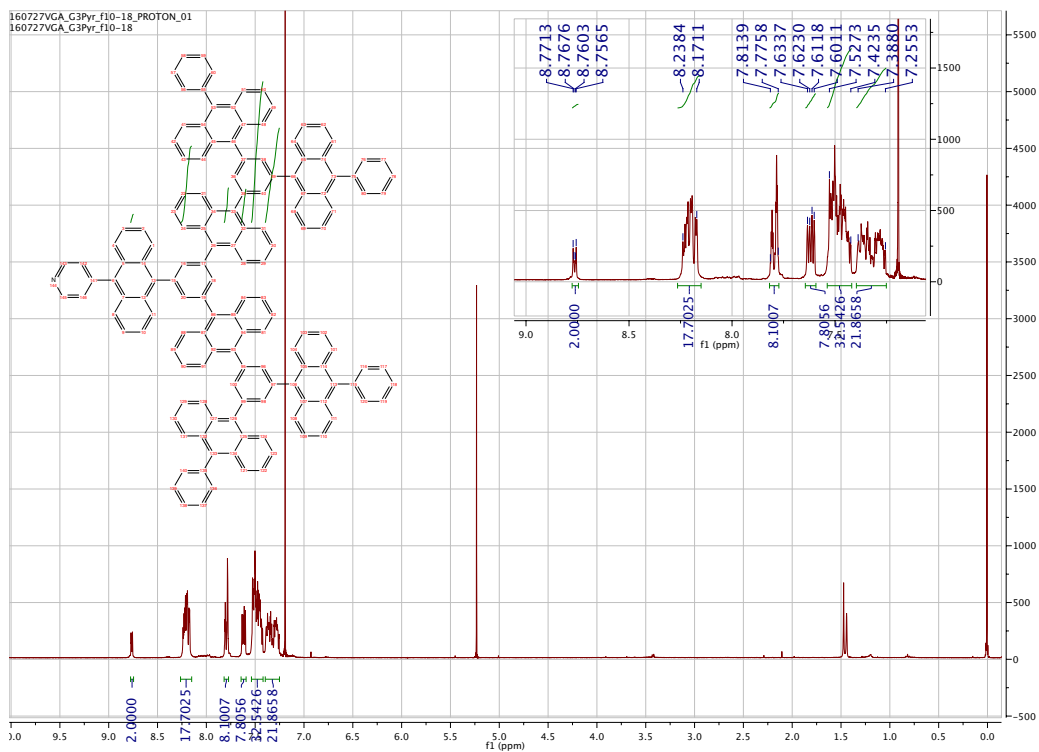


Figure S6: ^1H NMR of 7

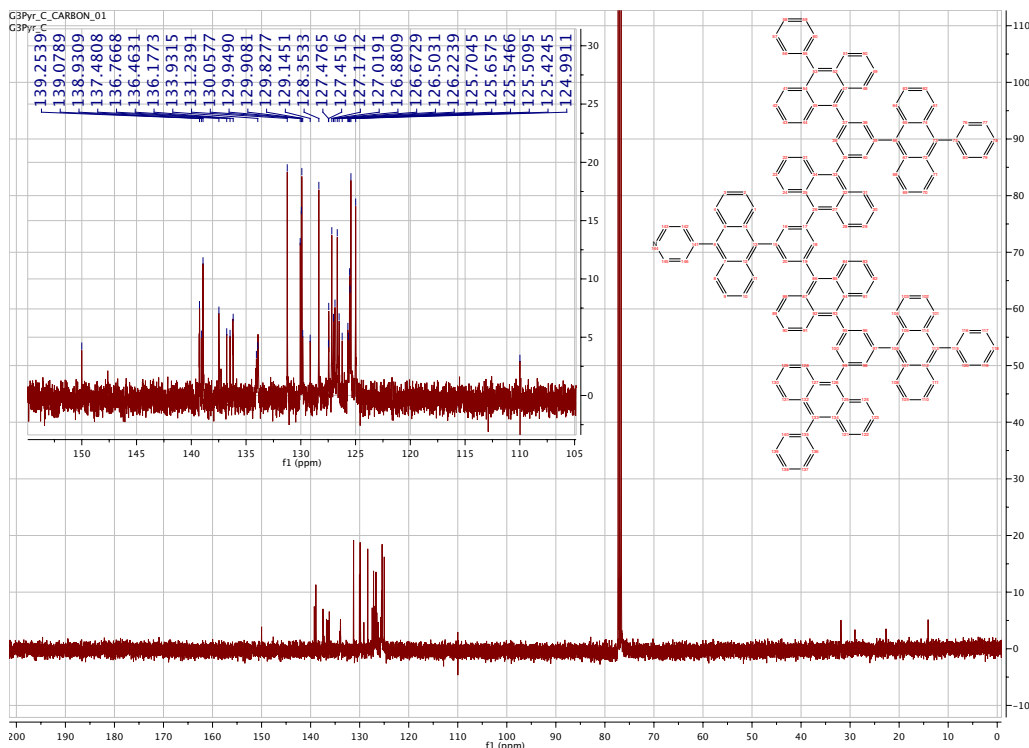


Figure S7: ^{13}C NMR of **7**

2 Binding dynamics and SVD analysis

The binding constant of the pyridine derivatives to **RuOEP(CO)** is determined by spectrophotometric titration.^{S4} The coordination trend is monitored in the Q-band region of **RuOEP(CO)** (between 460 nm and 600 nm). The employed binding model is:

$$K = \frac{k_a}{k_d} = \frac{[PL]}{[P][L]} = \frac{[PL]}{([P]_0 - [PL])([L]_0 - [PL])} \quad (\text{S1})$$

where k_a is the rate constant for complex formation, k_d is the rate constant for complex dissociation, $[PL]$ denote concentration of complex, $[P]$ is the concentration of free porphyrin and $[L]$ is the concentration of the free ligand, whereas $[P]_0$ and $[L]_0$ are the total concentrations of porphyrin and ligand respectively. Equation S2 show the analytical solution to

Equation S1.

$$[PL] = \frac{K[P]_0 + K[L]_0 + 1 - \sqrt{(K[P]_0 + K[L]_0 + 1)^2 - 4K^2[P]_0[L]_0}}{2K} \quad (\text{S2})$$

Since information about the degree of coordination is present both in amplitude and spectral shift of the absorption spectra, a Singular Value Decomposition (SVD) analysis is conducted as described elsewhere.^{S1,S4} Figure S8 shows the absorption and predicted spectra for the complex formation with ligands **2-7**. The obtained binding constants, K_{bind} and the degree of binding at a 1:1 ratio of P and L, is summarized in Table S1.

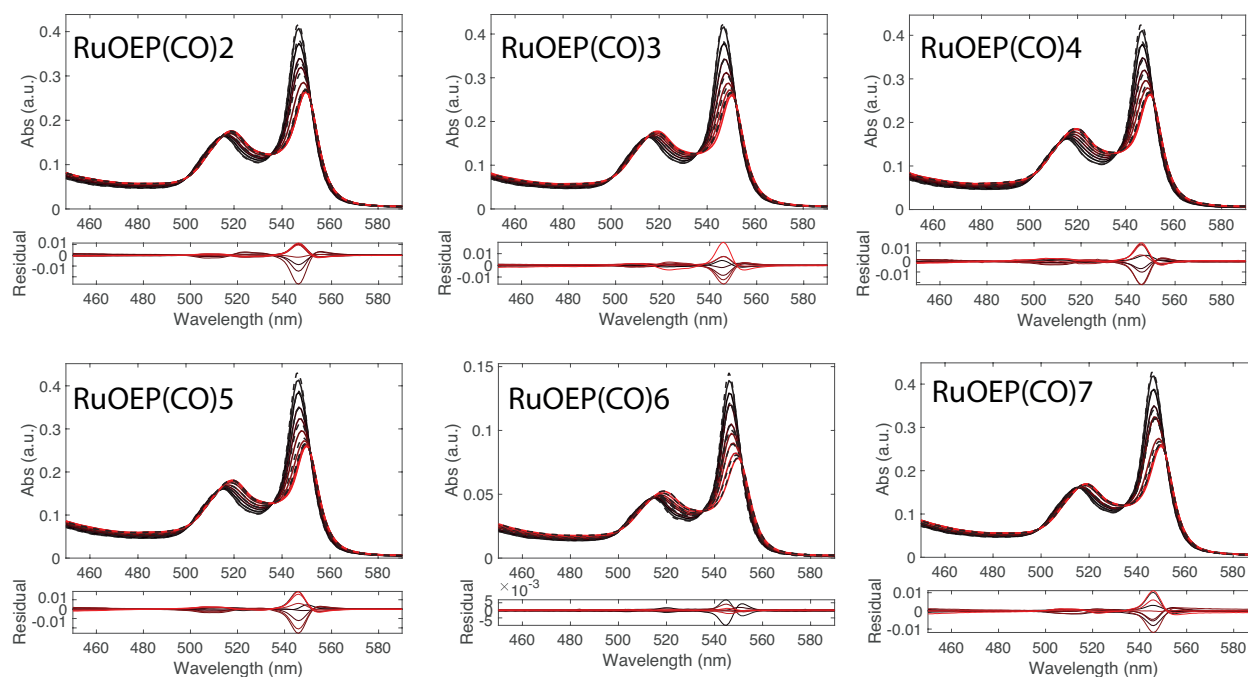


Figure S8: Shift in **RuOEP(CO)** (0.1 mM) absorption as ligands **L = 2-7** are added (0-0.15 mM) to form complex **RuOEP(CO)L**. Measured (dashed) and predicted (solid) spectra with residual below. Titration progression from black to red spectra.

Table S1: Binding constants, K_{bind} , and degree of binding for a 1:1 mixture of porphyrin and ligand (total porphyrin concentration is 0.1 mM).

Ligand	K_{bind} ($\times 10^6$ M $^{-1}$)	Fraction Bound (%)
1	12.9	91
2	53.8	96
3	1.8	81
4	7.0	90
5	9.2	91
6	3.9	86
7	7.8	90

3 Triplet Energy Transfer Dynamics

Phosphorescence spectra of **RuOEP(CO)Pyr** is shown in Figure S9. Minor impurities of the freebase porphyrin **OEP** was observed through fluorescence peaks at 570 nm and 624 nm, these peaks were not observed in phosphorescence spectra recorded with a 40 μ s delay.

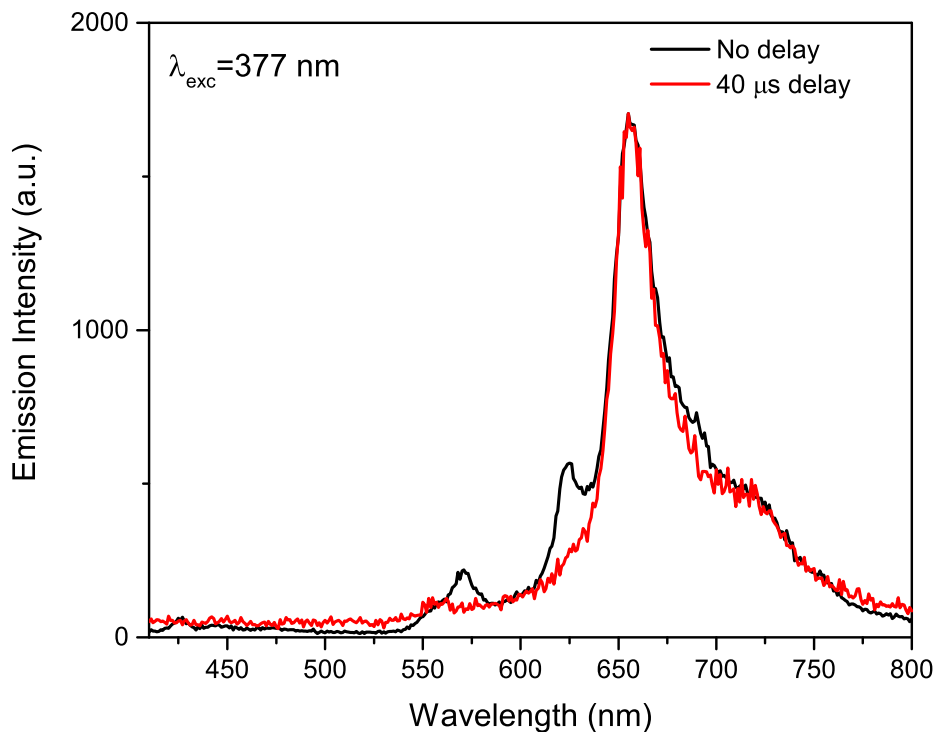


Figure S9: Phosphorescence spectra of **RuOEP(CO)Pyr**, excited at 377 nm and recorded with 0 μ s delay (black) and 40 μ s delay (red).

The quantum yield of phosphorescence, Φ_p is defined by the rate of phosphorescence over

the rate of excitation, as seen in Equation S3.

$$\Phi_p = \frac{k_r[{}^3P^*]}{k_{ex}[{}^1P]} \quad (\text{S3})$$

were k_r is the rate of radiative decay from the triplet state, k_{ex} is the rate of excitation and $[{}^iX]$ is the concentration of species X (P for porphyrin or L for ligand) in spin-state i (1 for singlet and 3 for triplet), the asterisk denotes an excited state. Further, assuming an intersystem crossing yield of 100%, the coupled rate equations shown in Equations S4-S6 describe the triplet energy dynamics in the system:

$$\frac{d[{}^1P^*]}{dt} = -k_{isc}[{}^1P^*] + k_{ex}[{}^1P] \quad (\text{S4})$$

$$\frac{d[{}^3P^*]}{dt} = k_{isc}[{}^1P^*] - k_{TP}[{}^3P^*] - k_{TET}[{}^3P^*] + k_{bTET}[{}^3L^*] \quad (\text{S5})$$

$$\frac{d[{}^3L^*]}{dt} = k_{TET}[{}^3P^*] - k_{bTET}[{}^3L^*] - k_{TL}[{}^3L^*] \quad (\text{S6})$$

were k_{TET} is the rate for TET from porphyrin (P) to a bound ligand, k_{bTET} is the rate for back TET from ligand (L) to porphyrin, k_{TP} is the rate for intrinsic decay of the porphyrin and k_{TL} is the rate of intrinsic decay of the ligand. Assuming steady state conditions the following three relations are obtained:

$$k_{ex}[{}^1P] = k_{isc}[{}^1P^*] \quad (\text{S7})$$

$$k_{isc}[{}^1P^*] = k_{TP}[{}^3P^*] + k_{TET}[{}^3P^*] - k_{bTET}[{}^3L^*] \quad (\text{S8})$$

$$[{}^3L^*] = \frac{k_{TET}[{}^3P^*]}{k_{bTET} + k_{TL}} \quad (\text{S9})$$

From the relations in Equations S7-S9 and Equation S3 one obtains Equation 3 in the main manuscript.

3.1 Transient Absorption Spectra

The transient absorption spectra of **RuOEP(CO)L** complexes with ligands **L=1, 3, 6** and **7** are shown in Figure S10. Spectra are recorded with a CCD camera and the decays are

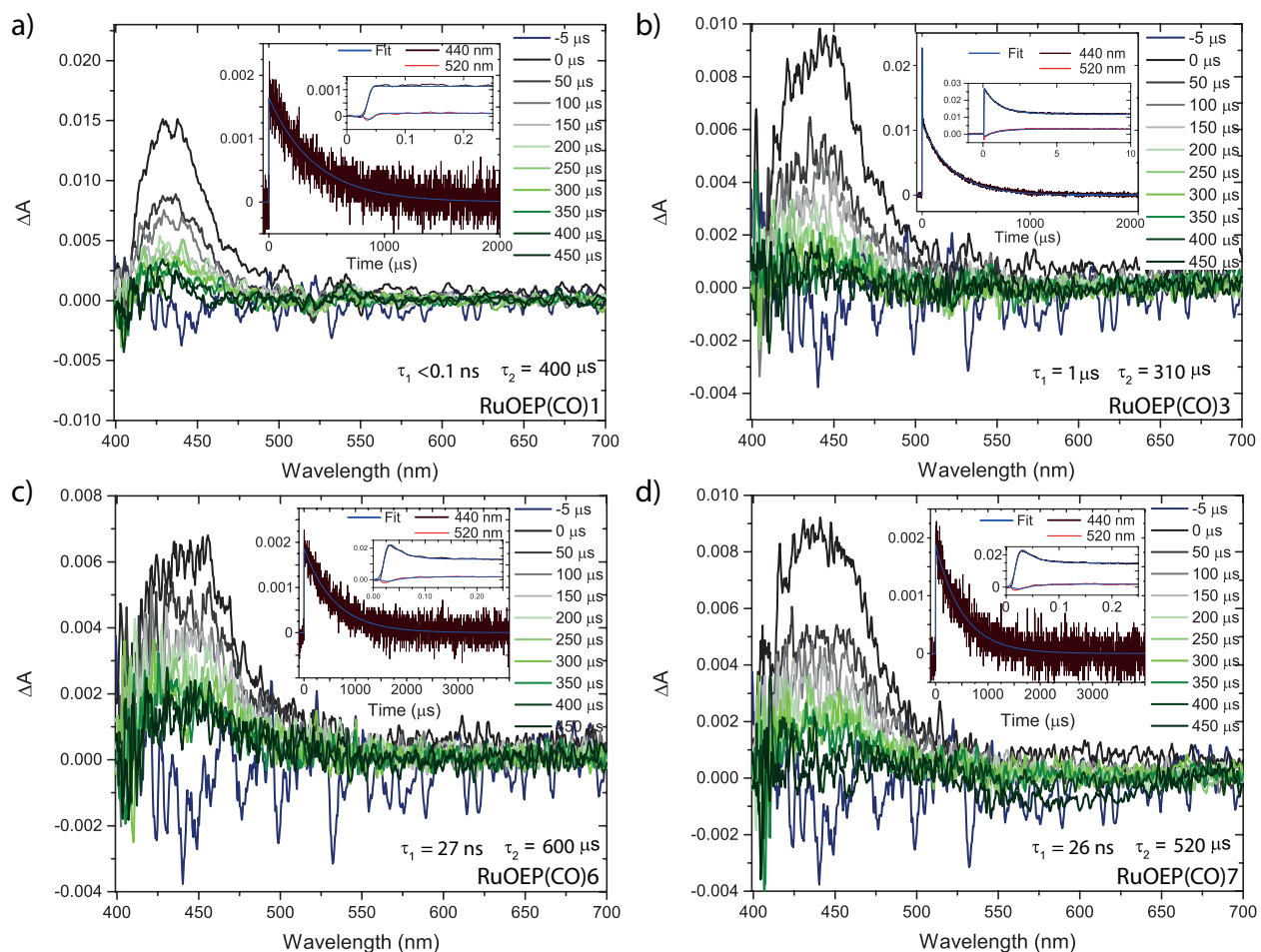


Figure S10: Transient absorption spectra of a) **RuOEP(CO)1**, b) **RuOEP(CO)3**, c) **RuOEP(CO)6** and d) **RuOEP(CO)7**. All samples excited at 550 nm.

recorded using an 5-stage PMT coupled to an oscilloscope, as described in the experimental section. The decay of the T_1-T_n absorption is recorded at 440 nm and the ground state bleach is monitored at 520 nm. The two decays (at 440 nm and 520 nm) of **RuOEP(CO)Pyr** were fit globally to a monoexponential decay, yielding a decay constant of 20.2 μs . The short decay times of ligand complexes **RuOEP(CO)L**, **L=1-4** and **6-7**, were extracted from global fits to the short time window decays at 440 nm and 520 nm. The long time

constant corresponding to the ligand triplet decay is obtained from fits at 520 nm with the short decay constant fixed.

For the complex with the longest bridge, $\mathbf{L} = \mathbf{5}$, the small amplitude of the ligand $T_1 - T_n$ absorption relative the porphyrin signal makes it difficult to extract the long ligand triplet lifetime. Therefore the decay of the porphyrin triplet absorption ($T_1 - T_n$) is first fit to a monoexponential decay yielding a decay constant of 13 μs , resulting in a reasonable fit for the majority of the decay, but significantly deviating at longer times. The obtained decay time is then fixed and the long lived decay from the ligand $T_1 - T_n$ absorption can be fit. The long decay constant is then fixed and the short decay is fit. The process is repeated until a satisfactory fit and reasonable lifetimes are obtained. All fits are done by deconvolution fitting assuming a 7 ns Gaussian shaped laser pulse.

3.2 Time resolved Phosphorescence

The time resolved phosphorescence and fits to mono- ($\mathbf{RuOEP}(\text{CO})\mathbf{L}$, $\mathbf{L}=\text{Pyr},\mathbf{1-3}$ and $\mathbf{6-7}$) and biexponential decays ($\mathbf{RuOEP}(\text{CO})\mathbf{L}$, $\mathbf{L}=\mathbf{4}$ and $\mathbf{5}$) are shown in Figure S11.

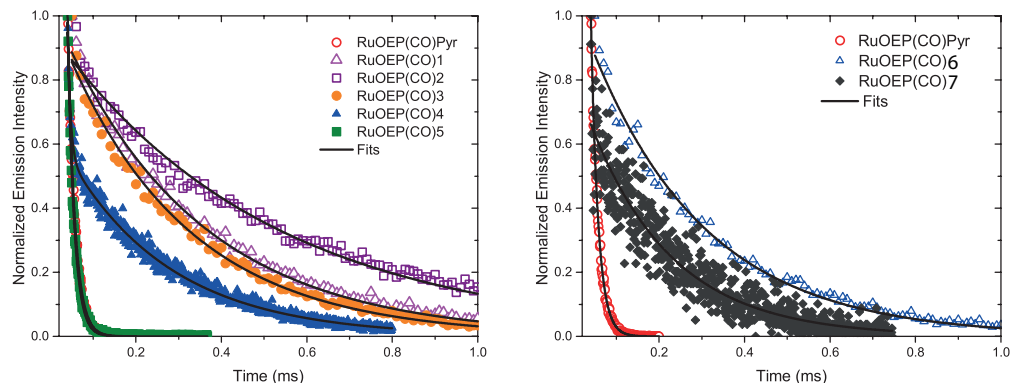


Figure S11: Phosphorescence decay of complexes $\mathbf{RuOEP}(\text{CO})\mathbf{L}$, excited at 405 nm and recorded at 650 nm. a) Decays of complexes with bridged ligands $\mathbf{1-5}$ and b) dendrimeric ligands $\mathbf{6}$ and $\mathbf{7}$.

4 Singlet Energy Transfer

Fluorescence decays with lifetimes shorter than 50 ps were measured on a streak camera system using a ps Ti:Sapphire laser tuned to 370 nm as described in the methods section. The fluorescence decay curves were extracted from the streak camera images by averaging the 440-450 nm emission wavelength range. Similarly, to estimate the instrument response function (IRF) of the system the scattering from a LUDOX colloidal silica solution was measured by averaging the 368-372 nm region. The IRF was fitted to a Gaussian function and the width (FWHM) was estimated to vary between 4-6 ps. The fluorescence decays were fitted to biexponential functions convoluted with the appropriate Gaussian to represent the impulse response. Lifetimes and amplitudes were optimized while keeping the width of the IRF constant. The optimized short lifetime represented the rate constant for singlet energy transfer and the long lifetime was kept fixed to the value determined (by TCSPC) for the unquenched, free ligand. For the **RuOEP(CO)3** complex the lifetime was shorter than the width of the Gaussian IRF and the lifetime was therefore estimated by a slightly alternative method as described in section 1.4 of the main article.

4.1 Förster Resonance Energy Transfer

The rate for Förster resonance energy transfer, k_{FRET} can be calculated from Equation S10

$$k_{FRET} = \frac{1}{\tau_0} \left(\frac{R_0}{R} \right)^6 \tag{S10}$$

where τ_0 is the intrinsic decay of the donor, R_0 is the Förster distance where the energy transfer is 50% efficient and R is the actual distance between donor and acceptor. We further have that $k_{FRET} = \frac{1}{\tau} - \frac{1}{\tau_0}$, which together with Equation S10 gives:

$$\log(k_{FRET}\tau_0) = \log\left(\frac{\tau_0}{\tau} - 1\right) = 6\log(R_0) - 6\log(R) \tag{S11}$$

Therefore, in a double logarithmic plot with fixed slope = -6, the intercept should be $6\log R_0$ as seen in Equation S11. With known spectral overlap integral, the orientation factor κ^2 can be estimated (if considered independent on bridge length) from Equation S12.

$$R_0 = 0.211(\kappa^2 n^{-4} \Phi_D \int_0^\infty F_D(\lambda) \epsilon_A(\lambda) \lambda^4 d\lambda)^{\frac{1}{6}} \quad (\text{S12})$$

From the fit, shown in Figure S12, with fixed slope of -6 R_0 is 50Å and $\kappa^2 = 1.59$. The fit with optimized slope gives an exponent of 5.4, slightly less than 6, possibly indicating a through bond (mediated) contribution to the singlet energy transfer, see main text for further discussion

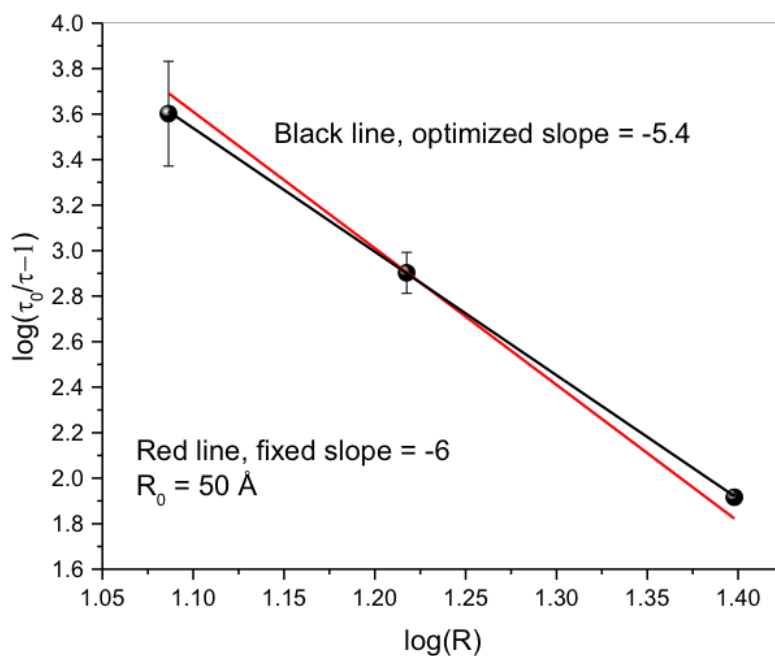


Figure S12: Double logarithmic plot of the singlet energy transfer rates ($k_{FRET}\tau_0$) as function of donor-acceptor distance (R) for the linear bridged systems (**RuOEP(CO)L**, L=3-5). Linear fits to the data points either with fixed slope (-6) or with optimized slope (-5.4) are shown with red or black lines, respectively.

4.2 Charge Transfer

The driving force for charge transfer in the current system was calculated according to the Marcus-Rehm-Weller Equation, and neglecting the Coulombic terms:

$$\Delta G^0 = E_{D/D^+} - E_{A/A^-} - E_{00} \quad (\text{S13})$$

where E_{D/D^+} is taken to be the redox potential in acetonitrile of **RuOEP(CO)Pyr** (0.66 V),^{S5} E_{A/A^-} is the redox potential of 9,10-diphenylanthracene (-1.83 V)^{S6} in acetonitrile and E_{00} is the excitation energy, taken to be 1.9 eV for the triplet state of **RuOEP(CO)**. With these numbers a positive ΔG^0 of 0.59 eV is obtained, indicating that electron transfer from the **RuOEP(CO)L** triplet state is unlikely in the studied systems. Since our systems are studied in toluene and ΔG^0 is calculated for acetonitrile it is expected that ΔG^0 is actually greater than 0.59 eV in the current system.

Comparing the calculated energy of the charge separated state (**RuOEP⁺(CO)L⁻**, 2.49 eV) to the energy of the ligand excited singlet state (**RuOEP(CO)¹L***, 3.10 eV) there seems to be a driving force for hole transfer ($\Delta G^0 = -0.6$ eV). Thus, if the destabilization of **RuOEP⁺(CO)L⁻** in toluene is less than 0.6 eV hole transfer would be possible from **RuOEP(CO)¹L***.

5 Upconversion Measurements

Upconverted emission intensity as a function of excitation intensity is plotted on a log-log scale in Figure S13 to verify the two regions of intensity dependence; a linear dependence at high excitation intensities and a quadratic dependence at lower excitation intensities.

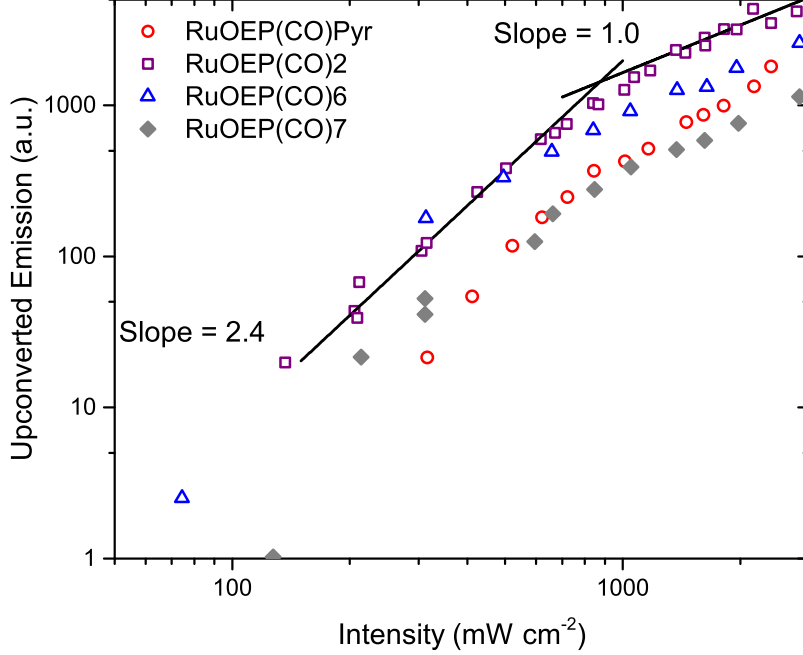


Figure S13: Excitation intensity dependence of the upconverted emission. Samples excited at 532 nm and intensity varied with a graded ND filter. Linear (slope ~ 1) and quadratic (slope ~ 2) fits are obtained for all four samples, for clarity only slope lines for **RuOEP(CO)2** are shown.

5.1 Effect of Extending the Triplet Lifetime of the Sensitizer

The upconversion quantum yield Φ_{UC} is a product of the efficiencies, Φ_i , of all involved processes, as described in Equation S14:

$$\Phi_{UC} = \Phi_{ISC}\Phi_{TET}\Phi_{TTA}\Phi_{FA} \quad (\text{S14})$$

where ISC, TET, TTA and FA denote intersystem crossing, triplet energy transfer, and fluorescence from the annihilator, respectively. In the studied UC systems, the differences are expected to only affect the TET efficiency, Φ_{TET} . From the Stern-Volmer relation, Equation S15, Φ_{TET} can be estimated from Equation S16.

$$\frac{\tau_0}{\tau} = 1 + k_q\tau[Q] \quad (\text{S15})$$

k_q is the bimolecular quenching constant, τ_0 is the lifetime of the sensitizer alone, and τ is the lifetime of the sensitizer in the presence of quencher.

$$\Phi_{TET} = 1 - \frac{\tau}{\tau_0} \quad (\text{S16})$$

In the current TTA-UC system, the quencher is the annihilator 9,10-diphenylanthracene, DPA. For metal porphyrins, like the palladium and platinum analogues **PdOEP** and **PtOEP**, with an triplet energy about 0.2 eV higher than that of DPA, the bimolecular quenching constant, k_q , is diffusion limited to about $2 \times 10^9 \text{ M}^{-1}$.^{S1,S7} In the case of a smaller driving force and more close to isoenergetic triplet energy alignment, for example **ZnOEP** and DPA, k_q is lower, about $0.8 \times 10^9 \text{ M}^{-1}$. When comparing Φ_{TET} between **RuOEP(CO)Pyr** and **RuOEP(CO)L** we assume that both **RuOEP(CO)Pyr** and **RuOEP(CO)2** are quenched with a k_q similar to that of **ZnOEP** as there is only a 0.1 eV driving force from **RuOEP(CO)Pyr** and for **RuOEP(CO)2** and DPA the triplet energies are isoenergetic. Figure S14 shows the dependence of Φ_{TET} on the quencher concentration for the two cases of sensitizers with triplet lifetimes of 20 μs and 420 μs , representing the case of **RuOEP(CO)Pyr** and **RuOEP(CO)2**, respectively. As can be seen, the TET is expected to be more efficient for the long lived sensitizer with a triplet lifetime of 430 μs , especially at low quencher concentrations $< 0.2 \text{ mM}$.

References

- (S1) Gray, V.; Börjesson, K.; Dzebo, D.; Abrahamsson, M.; Albinsson, B.; Moth-Poulsen, K. PorphyrinAnthracene Complexes: Potential in TripletTriplet Annihilation Upconversion. *J. Phys. Chem. C* **2016**, *120*, 19018–19026.
- (S2) Börjesson, K.; Gilbert, M.; Dzebo, D.; Albinsson, B.; Moth-Poulsen, K. Conjugated anthracene dendrimers with monomer-like fluorescence. *RSC Adv.* **2014**, *4*, 19846.
- (S3) Dzebo, D.; Börjesson, K.; Gray, V.; Moth-Poulsen, K.; Albinsson, B. Intramolecular

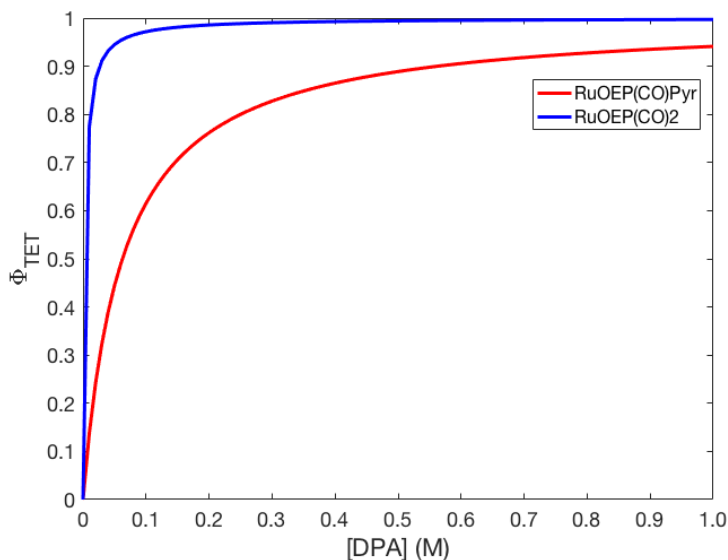


Figure S14: The triplet energy transfer efficiency, Φ_{TET} as a function of quencher concentration, [DPA]. Red corresponds to **RuOEP(CO)Pyr** with 20 μs triplet lifetime and assuming a bimolecular quenching constants of $0.8 \times 10^9 \text{ M}^{-1}$. Blue illustrates the case for a sensitizer with a longer lifetime of 430 μs the same bimolecular quenching constant.

Triplet-Triplet Annihilation Upconversion in 9,10- Diphenylanthracene Oligomers and Dendrimers. *J. Phys. Chem. C* **2016**, *120*, 23397–23406.

- (S4) Kubista, M.; Sjoback, R.; Albinsson, B. Determination of Equilibrium Constants by chemometric Analysis of Spectroscopic Data. *Anal. Chem.* **1993**, *65*, 994–998.
- (S5) Kadish, K. M.; Tagliatesta, P.; Deng, Y. J.; Bao, L. Y. Evaluation of Electron-Transfer Sites in Ruthenium(II) Octaethylporphyrin Complexes of the Type (OEP)Ru(CO)(L). *Inorg. Chem.* **1991**, *30*, 3737–3743.
- (S6) Haynes, W. M., Ed. *CRC Handbook of Chemistry and Physics*, 95th ed.; pp 5–85.
- (S7) Gray, V.; Dreos, A.; Erhart, P.; Albinsson, B.; Moth-poulsen, K.; Abrahamsson, M. Loss channels in Triplet-Triplet Annihilation Photon Upconversion: Importance of Annihilator Singlet and Triplet Surface Shapes. *Phys. Chem. Chem. Phys.* **2017**, *19*, 10931–10939.